

## ARTICLE OPEN



# Missense variants in *DPYSL5* associated with neurodevelopmental disorders and brain malformations cause impaired neuronal maturation in vitro

Florence Desprez<sup>1,2,22</sup>, Solène Remize<sup>1,2,22</sup>, Liberty François-Moutal<sup>3</sup>, Dévina C. Ung<sup>1</sup>, Audrey Dangoumau<sup>1</sup>, Sylviane Marouillat<sup>1</sup>, Joanna Kennedy<sup>4</sup>, Karen J. Low<sup>4,5</sup>, Camille Kumps<sup>6</sup>, Sheila Unger<sup>7</sup>, Boris Keren<sup>8</sup>, Jean-Madeleine de Sainte Agathe<sup>8</sup>, Céline Poirsier<sup>9</sup>, Ghayda M. Mirzaa<sup>10,11,12</sup>, Kimberly A. Aldinger<sup>10,12,13</sup>, Gaetan Lesca<sup>14,15</sup>, Valentin Ruault<sup>16</sup>, Candice R. Finnilla<sup>17</sup>, Whitley V. Kelley<sup>17</sup>, Donald R. Latner<sup>17</sup>, Sushma N. Guptha<sup>18</sup>, Annabelle Tuttle<sup>19</sup>, Ian Glass<sup>10</sup>, Wendy K. Chung<sup>10,20</sup>, Jennifer Cassidy Hayek<sup>10</sup>, Odile Boute<sup>21</sup>, Aubin Moutal<sup>3,23</sup>, Médéric Jeanne<sup>1,2,23</sup> and Frédéric Laumonnier<sup>1,2,23</sup>✉

© The Author(s) 2025

Neurodevelopmental disorders (NDD) with brain malformations have recently been associated with de novo variants in the *DPYSL5* gene, which encodes a member of the dihydropyrimidinase-like proteins family. Here, we aimed to understand its role in NDD by characterizing novel or recurrent de novo variants at the molecular and cellular levels. We collected clinical data on individuals in whom *DPYSL5* missense variants were identified through clinical genetic assessment of NDD or following the identification of brain malformations in fetuses. Functional analyses of wild-type and variant *DPYSL5* proteins were performed to evaluate their impact on in vitro neuronal development and maturation, using primary neuronal cultures from mouse embryonic brains or hiPSC-derived human neural stem cells. We describe six different missense variants in *DPYSL5* in nine individuals (including three fetuses), including the previously identified p.(Glu41Lys) recurrent mutation (in 2 individuals), a novel recurrent missense p.(Glu25Lys) de novo variant (in 3 individuals including 2 fetuses), and 3 novel candidates. Common features were developmental delay, intellectual disability, as well as brain malformations including agenesis of the corpus callosum for the N-terminal variants. Functional assays in differentiating mouse or human neuronal cultures revealed impairments in dendritic arborization, axonal elongation, and synaptic density. We thus expanded the functional characterization of *DPYSL5* variants in NDD with brain malformations, including at the fetal stage, highlighting a fundamental role of the *DPYSL5* gene in brain formation and functioning.

*Molecular Psychiatry*; <https://doi.org/10.1038/s41380-025-03364-8>

## INTRODUCTION

Neurodevelopmental disorders (NDDs) represent a highly heterogeneous group of early-onset cognitive and behavioral conditions affecting 2–3% of the general population [1]. NDDs are associated with a wide clinical and phenotypic heterogeneity, including syndromic and non-syndromic forms, as well as a significant genetic contribution, with more than 1,500 genes that have been implicated to date [2]. Within NDDs, brain malformations can be present and include abnormal cortical development [3], cerebellar dysplasia [4], or agenesis of the corpus callosum (ACC) which is present in 1–3% of individuals with impaired neurodevelopment [5].

DNA sequencing studies have led to the identification of candidate genes and pathogenic variants leading to ACC and NDDs through abnormal Semaphorin-mediated axonal guidance, and neuronal migration and specification [6]. Recently, several studies have reported the contribution of pathogenic de novo missense variants in the genes encoding members of the dihydropyrimidinase-like proteins family, associated with NDDs and ACC, such as *DPYSL2* (HGNC:3014) and *DPYSL5* (HGNC:20637) [7–9].

*DPYSL* proteins can coordinate cytoskeleton dynamics in young developing neuronal cells, by regulating filopodia formation, axonal

<sup>1</sup>Université de Tours, INSERM, Imaging Brain & Neuropsychiatry iBrain U1253, Tours, France. <sup>2</sup>Service de Génétique, CHRU de Tours, Tours, France. <sup>3</sup>Department of Pharmacology and Physiology, School of Medicine, St. Louis University, St. Louis, MO, USA. <sup>4</sup>Clinical Genetics, University Hospitals Bristol, Southwell St, Bristol, UK. <sup>5</sup>Centre for academic child health, Bristol Medical School, University of Bristol, Bristol, UK. <sup>6</sup>Division of Genetic Medicine, Lausanne University Hospital (CHUV), Lausanne, Switzerland. <sup>7</sup>Genetica, Lausanne, Switzerland. <sup>8</sup>Département de génétique, AP-HP, Sorbonne Université, Paris, France. <sup>9</sup>Department of Genetics, Reims University Hospital, Reims, France. <sup>10</sup>Department of Pediatrics, Division of Genetic Medicine, University of Washington School of Medicine, Seattle, WA, USA. <sup>11</sup>Department of Laboratory Medicine and Pathology, University of Washington School of Medicine, Seattle, WA, USA. <sup>12</sup>Brotman Baty Institute for Precision Medicine, Seattle, WA, USA. <sup>13</sup>Center for Integrative Brain Research, Seattle Children's Research Institute, Seattle, WA, USA. <sup>14</sup>Genetics Department, Hospices Civils de Lyon, Lyon, France. <sup>15</sup>Neuromyogène Institute, CNRS UMR 5261 INSERM U1315, Université Claude Bernard Lyon 1, Lyon, France. <sup>16</sup>Montpellier University, Reference Center for Rare Disease, Medical Genetic Department for Rare Disease and Personalized Medicine, CHU Montpellier, Montpellier, France. <sup>17</sup>HudsonAlpha Institute for Biotechnology, Huntsville, AL, USA. <sup>18</sup>Permanente Medicine, San Jose, CA, USA. <sup>19</sup>GeneDx, LLC, Gaithersburg, MD, USA. <sup>20</sup>Department of Pediatrics, Division of Genetics and Genomics, Boston Children's Hospital and Department of Pediatrics, Harvard Medical School, Boston, MA, USA. <sup>21</sup>Clinique de Génétique, Université de Lille, ULR7364 RADEME, CHU Lille, Lille, France. <sup>22</sup>These authors contributed equally: Florence Desprez, Solène Remize. <sup>23</sup>These authors jointly supervised this work: Aubin Moutal, Médéric Jeanne, Frédéric Laumonnier. ✉email: frederic.laumonnier@inserm.fr

Received: 16 September 2024 Revised: 21 October 2025 Accepted: 6 November 2025

Published online: 24 November 2025

guidance, neurite outgrowth and establishment of neuronal polarity, through direct interaction with tubulin and actin [7]. For instance, the tubulin-DPYSL5 interaction leads to inhibition of microtubule polymerization and consequently negative regulation of dendritic growth in cultured neurons, whereas DPYSL2 promotes dendritic elongation [7, 10, 11]. The DPYSL5 variants p.(Glu41Lys) and p.(Gly47Arg) cause loss of the inhibitory regulation of DPYSL5 on dendritic growth in primary neuronal cultures from mouse embryonic brain tissue, and the proposed pathophysiological mechanism was a significant decrease of the interaction ability between each mutated DPYSL5 form and the MAP2 and TUBB3 cytoskeleton-associated proteins [8].

In the present study, we expand the contribution of *DPYSL5* in NDD with the report of novel missense variants associated with NDD and brain malformations including ACC, as well as the description of additional cases with the pathogenic recurrent NM\_020134.4: c.121 G > A, p.(Glu41Lys) variant. We also provide functional evidence for the impact of pathogenic variants at the cellular level (abnormal in vitro neuronal development, affecting either axonal or dendritic elongation processes) using mouse and human neuronal models. We describe that synaptic defects present in mature hippocampal neurons overexpressing DPYSL5 with the missense variant located at the N-terminal domain (p.Glu25Lys, p.Glu41Lys, and the p.Gly47Arg variant that is associated with Ritscher-Schinzel syndrome – MIM #619435), suggesting that DPYSL5 also contributes to synapse homeostasis at later neurodevelopmental stages. These findings suggest that DPYSL5 represents a genetic form of NDD with corpus callosum dysgenesis.

## MATERIALS/SUBJECTS AND METHODS

The following sections are expanded upon in Supplementary Methods.

### Clinical and genetic analyses

We collected biological and clinical data from nine individuals from nine unrelated families, through to a multicenter and international collaboration through GeneMatcher [12]. Inclusion in the study was based on the identification of a de novo *DPYSL5* variant, except for one adopted individual whose biological parents were not assessed (Table 1). Detailed clinical data including medical and developmental history, brain imaging and any other relevant medical information were collected through a standardized clinical form completed by referring physicians. Genetic analyses were performed at each clinical center through routine clinical and genetic diagnostic pipelines of exome or genome sequencing. DNA was extracted either from peripheral blood mononuclear cells (PBMC) or from amniotic cells for fetuses. The allelic frequency of each nucleotide variation was determined using gnomAD (v3.1 non neuro, and v4.1), and predicted deleterious impact on the protein was assessed by in silico prediction softwares, such as CADD, REVEL, ClinPred and alphaMissense [13–16]. The variants annotations were checked using Variant Validator [17], and are referenced to GRCh38, NM\_020134.4 and NP\_064519.2 reference sequence numbers (Supplementary Table 1).

### DPYSL5 expression plasmid and site-directed mutagenesis

Full-length human *DPYSL5* cDNA (GenBank AF264015) was amplified by PCR and inserted directionally into the pEGFP-C1 vector (Clontech), as previously described [8]. The six variants were generated by site-directed mutagenesis using the Q5® Site-Directed Mutagenesis Kit (New England Biolabs). The oligonucleotide primers sequences for each variant are indicated in Supplementary Table 2. The presence and the correct insertion of each nucleotide substitution on the GFP-DPYSL5 plasmid was confirmed by Sanger sequencing.

### Primary neuronal culture, transfection and immunocytochemistry

Hippocampal and cortical cultures were prepared from embryonic day 17.5 (E17.5) C57BL/6J WT mouse embryos (Janvier Labs) as previously described [18]. The developing neurons were transfected with pCAG-GFP and different plasmid constructs (WT or mutated forms of GFP-DPYSL5) using Lipofectamine 2000 (Invitrogen) with 1 µg of DNA/1.6 µl of L2000 diluted in Neurobasal medium (Invitrogen), either at 4 days after plating (day in vitro, DIV 4) to analyze neurite growth, or at DIV 11 to study synapses morphology and density. The transfection mix was added to cells and incubated for 4 h (37 °C, 5% CO<sub>2</sub>), then the transfection medium was replaced with a mix 1:1 of new complete culture medium and previously removed medium (conditioned medium) for neurons or only new medium for cell lines. Cells cultured on coverslips were fixed with a solution of paraformaldehyde 4%/sucrose 4% 72 h after transfection. Fixed neurons were blocked and permeabilized with blocking buffer containing donkey serum 10%/Triton X-100 0.2% in DPBS for 1 h and incubated 1 h in a similar solution (DPBS, 0.2% Triton X-100, 3% donkey serum) containing primary antibodies: Rabbit polyclonal anti-Tau Antibody (1/1000; Cat# 314003, Synaptic Systems), Mouse monoclonal anti-MAP2 antibody (1/200; Cat# M9942, Sigma-Aldrich), Mouse monoclonal anti-PSD95 (1/300; Cat# MA1-045, ThermoFisher Scientific). After several washes in DPBS, cells were incubated for 1 h with the following secondary antibodies diluted in same solution (DPBS, 0.2% Triton X-100, 3% donkey serum): Alexa Fluor™ 594 Donkey anti-mouse IgG (1/300; Cat# A-21203, ThermoFisher Scientific), Alexa Fluor™ 405 Goat anti-Rabbit IgG (1/300; Cat# A-31556, ThermoFisher Scientific). After 3 washes in DPBS, the stained neurons were mounted in ProLong Diamond Antifade reagent (ThermoFisher scientific).

### Culture of hiPSC and CRISPR-Cas 9 genome editing of the p.(Glu41Lys) recurrent variant

The control human induced pluripotent stem cell (hiPSC) line used for this study was the ASE-9211 line (Applied Stem Cell, CliniSciences). The cells have been authenticated by the provider and routinely tested for mycoplasma contamination. For culture, plates were pre-coated with 1X matrigel (ThermoFisher Scientific) diluted in DMEM/F12 (ThermoFisher Scientific) and 1X antibiotic-antimycotic (ThermoFisher Scientific). Cells were cultured in supplemented mTeSR1 medium (StemCell) with a change of medium every day. On days of thawing or passage of hiPSC, the medium was supplemented with 10 µM Rock inhibitor (Y-27632, Sigma-Aldrich). The cells were then genetically modified with CRISPR-Cas9 system (ICV-iPS core facility, Paris Brain Institute, ICM): a total of  $1 \times 10^6$  hiPSC were nucleofected with RNP complex (225 pmol of each RNA (crRNA, crRNA-ATTO+), 120 pmol of Cas9 protein and 2 nmol HR-template. The crRNA sequence used is as follows: CGCCAGG-GATCATGAGCTcGCGG. The positive clones were then validated by using PCR and Sanger sequencing, to confirm the insertion of the mutation (genotype <sup>WT/p.Glu41Lys</sup>), and the heterozygous state of the mutation. The detection of CNVs was performed using ICS-digital method (Stem Genomics).

### Generation of neural stem cells (NSC) and culture conditions

The hiPSC clones were dissociated into single cells and seeded at a density of 200,000 cells in a matrigel-coated 6-well plate. The following day, mTeSR1 was replaced by neuronal induction medium (Neurobasal Medium with 2% Neural Induction Supplement 50X, Thermo Fisher scientific). On day 7, differentiating cells were detached using accutase and resuspended in neural expansion medium (49% Neurobasal Medium, 49% Advanced DMEM/F12, 2% Neural Induction Supplement 50X, ThermoFisher scientific). Cells were maintained and expanded on pre-coated matrigel plates at a density of  $5 \times 10^4$  cells per cm<sup>2</sup>. Cells were

**Table 1.** Clinical features of the individuals with a missense variant in *DPYSL5*.

Individual	1	2	3	4	5	6	7	8	9
<b>Genetic data</b>									
GRCh38 (NC_000002.12)	g.26898572 G > A	g.26898572 G > A	g.26898572 G > A	g.26898620 G > A	g.26898620 G > A	g.26931662 G > T	g.26933300 G > T	g.26940143 C > T	g.26944777 G > A
c. (NM_020134.4)	c.73 G > A	c.73 G > A	c.73 G > A	c.121 G > A	c.121 G > A	c.692 G > A	c.757 G > T	c.1060 C > T	c.1562 G > A
p. (NP_064519.2)	p.(Glu25Lys)	p.(Glu25Lys)	p.(Glu25Lys)	p.(Glu41Lys)	p.(Glu41Lys)	p.(Arg231His)	p.(Ala253Ser)	p.(Arg354Cys)	p.(Arg521Gln)
Inheritance	heterozygous, de novo	heterozygous, de novo	heterozygous, de novo	heterozygous, de novo	heterozygous, de novo	n.a. (adopted)	heterozygous, de novo	heterozygous, de novo	heterozygous, de novo
<b>General data</b>									
Age at last examination	10 y	fetus (26 gw)	fetus (30 gw)	8 y	fetus (32 gw)	n.a.	2 y 2 m	8 y 6 m	4 y 6 m
Gender	F	M	M	M	M	M	M	M	F
Antenatal findings	CCA	CCA	CCA	CCA	CCA	SGA	-	-	SGA
Hypotonia	-	-	-	-	-	n.a.	-	+	+
Feeding difficulty	+	-	-	-	-	n.a.	-	+	+
Failure to thrive	+	-	-	-	-	n.a.	-	-	+
Microcephaly	-	n.a.	n.a.	n.a.	n.a.	n.a.	-	n.a.	-
Macrocephaly	-	n.a.	n.a.	n.a.	n.a.	n.a.	-	n.a.	-
Short stature	-	+	+	+	+	n.a.	-	-	+
<b>Neuro / development</b>									
Delayed development	+	+	+	+	+	+	+	+	+
Type (global, language, motor)	motor	global	global	global	global	language	language	language	global
Walking (age)	25 m	-	36 m	+	36 m	n.a.	15 m	12 m	> 36 m
Fine motor problem	-	-	-	+	+	n.a.	-	hemiplegia	+
1st words (age)	normal	normal	normal	24 m	24 m	n.a.	24 m	36 m	delay
ID	+	+	+	+	+	+	+	+	+
ASD	+	+	+	+	+	+	+	+	+
Behavioral problems	-	-	-	+	+	n.a.	-	+	n.a.
Epilepsy	-	-	-	-	-	n.a.	infantile spasms	-	-
Ataxia	+	+	+	+	+	n.a.	-	-	-
Muscle weakness	+	+	+	-	-	n.a.	-	all limbs	+
<b>Brain imaging</b>									
Corpus callosum agenesis	+	+	+	+	+	-	-	-	-
Cerebellar hypoplasia	-	-	-	+	+	-	-	-	+
Others	-	-	-	-	-	-	-	chiar 1 malformation	chiar 1 malformation

Table 1. continued

Individual	1	2	3	4	5	6	7	8	9
<b>Medical problems / congenital anomalies</b>									
Visual problems	myopia, strabismus, 4th nerve palsy in one eye			astigmatism		-	-	hyperopia, strabismus, adhesions in orbits found	decreased visual acuity
Gastro-intestinal problems	constipation			-		n.a.	-	constipation	dysphagia with thin liquids
Additional findings	2 natal teeth	n.a.	femoral length <5th percentile	bilateral orchidopexy for small undescended testes with hypogonadotrophic hypogonadism, bilateral ankle overpronation	n.a.	hypopigmented lesions	n.a.	PFO, sleep apnea (resolved), ankle hypermobility, deep set eyes with long palpebral fissures, widely spaced, multiple café-au-lait spots	bilateral ptosis, hypotonic facies

The empty sections represent clinical items that were not assessed in the fetuses (individuals 2, 3 and 5).

ASD autism spectrum disorder, CCA agenesis of the corpus callosum, F female, gw gestational week, ID intellectual disability, m month(s); M, male, n.a. not available, SGA small for gestational age, y year(s).

passed and treated overnight with 10  $\mu$ M Rock inhibitor to promote attachment until passage 4, when a pure Neural Stem Cells (NSC) culture was obtained.

### Immunocytochemistry and protein extraction on NSC

The NSC were labelled with MAP2 Antibody to specifically detect the neurites. The stained NSC were mounted in ProLong Diamond Antifade reagent with DAPI (Invitrogen). Neuronal proteins were extracted from NSCs and iPSC using N-Per lysis buffer (ThermoFisher Scientific) supplemented with 1% protease inhibitor (Halt™ Protease Inhibitor Cocktail 100X, EDTA-Free, ThermoFisher Scientific).

### Western blot

Protein samples were processed for SDS-PAGE conditions at 110 V for 1 h. SDS-PAGE gels were transferred to a PVDF membrane using the TransBlot Turbo transfer system (Bio-Rad) for 3 min (2.5 A, 25 V). The membrane was blocked for 1 h with 5% milk diluted in TBS-Tween (Tris Buffer Saline, ThermoFisher Scientific with 1% Tween 20, Sigma-Aldrich). The primary antibodies were incubated overnight at 4 °C in TBST buffer with 5% milk. After 3 washes in TBST, the membranes were incubated with the corresponding horseradish peroxidase (HRP)-coupled secondary antibodies for 1 h at room temperature. For normalization of protein levels, we used actin (antibody: anti- $\beta$ actin-peroxydase, 1/100000; Cat# A3854-200UL, Sigma-Aldrich) as a loading control. Membrane revelation by chemiluminescence was performed using the Clarity Western ECL kit (Bio-Rad) on the ChemiDoc Touch instrument (Bio-Rad). The following antibodies were used: Affinity-purified rabbit polyclonal anti-DPYSL5 (1/2000; kind gift from Pr Honnorat's lab [10]; Goat polyclonal antiserum anti-vGLUT1 (1/1000; Cat# 134307, Synaptic System); Monoclonal Mouse anti-PSD95 (1/100; Cat# MA1-045, ThermoFisher Scientific). The secondary antibodies were: Peroxidase conjugated anti-rabbit (1/2500; Cat# W401B, Promega), peroxidase conjugated anti-mouse (1/2500; Cat# W402B, Promega) and peroxidase conjugated anti-goat (1/2500; Cat# V8051, Promega).

### Image analysis

The cellular imaging study was performed using a laser-scanning confocal microscope SP-8 (Leica) and the software Leica Application Suite X (LAS X). Sequential acquisitions were made, and high-resolution z stack images of cells were taken with the X63 or 20X objective with optical section separation (z interval) of 0.2  $\mu$ m for the images of the dendritic spines (20X objective, z interval 0.3  $\mu$ m for the complete neuron). The length of NSC neurites was measured on images acquired at 40X, z interval 0.3  $\mu$ m. The cells included in the analysis had process <2 cell bodies in length [19]. The images were analyzed on maximum projections using with ImageJ Software. Three different portions of dendrites were taken within each neuron, and the number of dendritic spines was normalized to 10  $\mu$ m of dendrite length. Mature (mushroom and stubby) and immature (thin and filopodia) spines were differentiated according to two criteria: (1) the presence or absence of PSD95 protein labeling, and (2) head diameter > 0.6  $\mu$ m for mature (mushroom) spines or head diameter <0.6  $\mu$ m for immature thin spines [20].

### Statistical analysis

Statistical analysis was carried out using the GraphPad Prism 8.0 software (La Jolla, CA, USA). For the neuronal morphological study and the expression of variants, the data were analyzed using Kruskal Wallis Test followed by Dunn's multiple comparisons test. For the density of spines analysis, a Shapiro-Wilk normality tests determined data normality, the data were then analyzed using an ordinary one-way ANOVA followed by Tukey's multiple comparisons. To evaluate the ratio of mature and immature spines, Kruskal Wallis and Dunn's post-hoc tests were done. For the different experiments

that compared WT/WT NSC and <sup>WT/p.Glu41Lys</sup> NSC, Mann Whitney tests were performed. Statistical significance was defined as  $P < 0.05$ .

## RESULTS

### Clinical spectrum associated with DPYSL5 variants

The cohort included three male fetuses and six individuals aged up to 10 years old. All the living participants had developmental delays (6/6), predominantly in language (5/6), and mild to severe intellectual disability (5/5). Four individuals had autism spectrum disorder (ASD), and 2/4 had self-harm or temper tantrum-like behaviors. Two participants had ataxia and one had infantile spasms. Brain imaging revealed that two living participants had cerebral malformations including ACC and cerebellar hypoplasia, and two other ones had Chiari I malformation. The three fetuses, whose pregnancies were terminated, had ACC, also associated with hypoplasia of the vermis and agenesis of the olfactory bulbs in one fetus. Additional features are presented in Table 1 and in Supplementary Information (for 2 individuals).

Two participants, including one fetus, carried the recurrent de novo missense variant NM\_020134.4:c.121 G > A, p.(Glu41Lys) that we previously reported as associated with ID and ACC [8]. We identified a second recurrent de novo variant, NM\_020134.4:c.73 G > A, p.(Glu25Lys) present in three individuals of our series, all with ACC and ID.

We also report four other novel missense variants, NM\_020134.4:c.692 G > A, p.(Arg231His); c.757 G > T, p.(Ala253Ser); c.1060 C > T, p.(Arg354Cys) and c.1562 G > A, p.(Arg521Gln). All variations are de novo, except for one adopted patient (p.Arg231His) for whom inheritance data were not available.

The candidate variants were initially absent from the control population database Genome Aggregation Databases (gnomAD v.3.1.2, non-neuro subset), with the exception of c.1562 G > A, which was found once (Supplementary Table 1). However, the last release of gnomAD (v4.1) revealed that c.692 G > A is found in 5 individuals (5/1613890 alleles, all from the UKBiobank subset); c.1060 C > T is found in 1 individual (1/1614108 alleles); c.1562 G > A variant is found in 4 individuals (4/1614032 alleles including 2 from the UKBiobank subset) (Supplementary Table 1).

According to the American College of Medical Genetics (ACMG) and Genomics and Association for Molecular Pathology criteria [21], c.73 G > A, c.121 G > A, c.757 G > T, c.1060 C > T would be thus classified as pathogenic, and the c.692 G > A and c.1562 G > A variants would be considered as of uncertain significance, although the proposed criteria application and variant classification do not necessarily reflect the criteria and classification of the clinical testing laboratories involved in the study (Supplementary Table 1).

### The DPYSL5 variants are clustered in distinct structural protein domains

We next followed a structure-based approach to better evaluate the location of DPYSL5 missense variants, by using crystal structural DPYSL5 protein model (PDB 4b90), and AlphaMissense prediction tool (Fig. 1A, Supplementary Table 1) [15, 22]. The predicted impact of DPYSL5 variants p.Glu41Lys (E41K), p.Gly47Arg (G47R), p.Arg231His (R231H), and p.Arg354Cys (R354C) was classified as pathogenic, whereas the p.Glu25Lys (E25K) variant was classified as ambiguous, and the p.Ala253Ser (A253S) and p.Arg521Gln (R521Q) variants were classified as

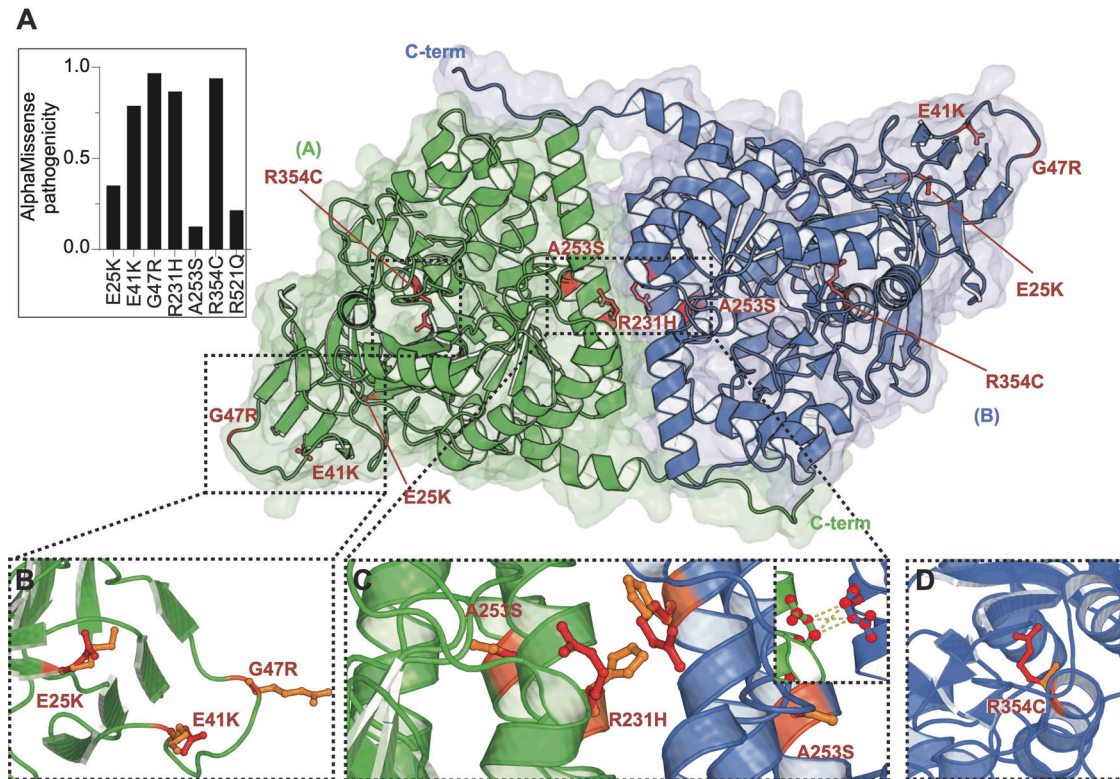


**Fig. 1** Mapping of the variants on the three-dimensional structure of DPYSL5 dimer. **A** Ribbon representation overlaid on smoothed surface with key residues shown as sticks (red). Letters in parentheses indicate subunits (PDB: 4b90). Insert: Predicted pathogenicity of each mutation by AlphaMissense. Close up views of the indicated residues (in red) overlaid with their replaced residue (in orange), with the surrounding protein shown in green ribbon representation as follows **B** E25K (p.Glu25Lys), E41K (p.Glu41Lys) and G47R (p.Gly47Arg), **C** Close up view of the Arg231 (R231) residues at the dimer interface making several hydrogen bonds (dash, yellow). **D** View of p.Arg354Cys (R354C) position. The p.Arg521 (R521) is not represented here because of its localization outside of the reported crystal structure. Images were generated on PyMol.

benign (Fig. 1A, Supplementary Table 1). Substitution of Arg231 residue with histidine could impair dimerization by abolishing hydrogen bonding. Residue Arg521 is localized in a disordered region of the protein, and the p.Glu41Lys (E41K) and p.Gly47Arg (G47R) are localized in loops, which impact interactions with binding partners of DPYSL5 (Fig. 1B) [8]. However, they are not implicated in multimerization (not shown). Residues Ala253 and Arg354 are buried within the structure and localized within alpha helices (Fig. 1C). Because of its low pathogenicity score, p.Ala253Ser may not have a large effect on the structure of DPYSL5. However, since p.Arg354Cys has a high score of pathogenicity, it is possible that the protein structure is affected by the mutation resulting in stability issues (Fig. 1D).

### Altered dendritic or axonal elongation processes in young developing neuronal cultures overexpressing candidate de novo DPYSL5 variants

The DPYSL5 protein has been described as being involved in the fine regulation of axonal and dendritic elongation processes in the young developing neuronal cells, through an inhibitory action mechanism competing with the promoting action of DPYSL2 [7]. We previously found that both p.(Glu41Lys) and p.(Gly47Arg) variants led to the loss of this specific function, which was associated with a decreased interaction between DPYSL5 and MAP2 or TUBB3 proteins [8]. Considering these findings, we assessed four out of the five novel candidate de novo DPYSL5 variants, by transfecting GFP-DPYSL5 wild-type (WT) or variant expression plasmids in young primary hippocampal neurons (at 4 days of culture) in which axonal and dendritic elongation are active. Since we focused our functional analysis on de novo variants, we did not assess the p.(Arg231His) variant because of its inheritance status remained undetermined as the patient was adopted. Importantly, each DPYSL5-WT and variant expression plasmid constructs was assessed in HEK293T cell lines using transfection and western blotting experiments (Supplementary Fig. 1). As shown in Fig. 2, the overexpression of GFP-DPYSL5-WT caused a decrease of the total dendrite length (Fig. 2A, B) but not total axonal length (Fig. 2A, C), when compared to the neurons transfected with pCAG-GFP plasmid (negative control), which recapitulates its physiological inhibitory action on dendrite elongation. We then found that the axonal total length was not altered by the p.(Glu25Lys), p.(Ala253Ser) and p.(Arg521Gln) variants, unlike the p.(Arg354Cys) variant for which a significant decrease of axonal length was observed (Fig. 2C). Regarding the dendrite total length, while we observed (as a positive control) the physiological inhibitory regulation of GFP-DPYSL5-WT on dendrite elongation compared to neurons expressing only the GFP, we discovered that the p.(Glu25Lys), p.(Ala253Ser) and p.(Arg521Gln) variants did not abolish the dendrite outgrowth, suggesting an alteration of DPYSL5 function (Fig. 2B). Conversely, the p.(Arg354Cys) variant overexpression led to reduced dendrite total length, similarly to WT-DPYSL5 (Fig. 2B).

Consequently, our cellular experiments indicate that the p.(Glu25Lys), p.(Ala253Ser) and p.(Arg521Gln) variants impair dendrite elongation and outgrowth, in line with what we previously described for the p.(Glu41Lys) and p.(Gly47Arg) mutations. Furthermore, we describe a novel pathophysiological mechanism associated with the p.(Arg354Cys) variant, which has a major effect on axonal elongation. It may be likely that the arginine to cysteine substitution creates novel disulfide bonds and potentially destabilize the overall secondary structure of DPYSL5, which might explain the decreased expression level of DPYSL5-Arg354Cys protein in HEK293 cell lines (Supplementary Fig. 1). Interestingly, we also found a strongly decreased expression level of endogenous DPYSL5 in total protein extracts from HEK293 cells overexpressing the p.(Arg354Cys) variant, suggesting that the conformation and stability of WT/Arg354Cys DPYSL5 dimers would be impaired and lead to a possible protein

degradation and loss of expression (i.e. function) impact. We then tested if the variants impact DPYSL5 interaction with cytoskeletal proteins, as previously described for the p.(Glu41Lys) and p.(Gly47Arg) variants. However, our in vitro experiments revealed no significant alteration of its interaction ability with MAP2, DPYSL2 or  $\beta$ III-tubulin (Supplementary Fig. 2), suggesting that these residues, including the Glutamate 25, may not be located in a protein domain essential for this physiological action.

### The N-terminal DPYSL5 p.(Glu25Lys), p.(Glu41Lys) and p.(Gly47Arg) variants impair synaptic density and maturation

Besides its well-documented function in brain developmental architecture, such as the formation of the corpus callosum, it is also suggested that DPYSL5 might play a significant role in synaptic development and function. Indeed, in mature excitatory glutamatergic synapses, DPYSL5 can regulate the endocytosis of GluA2 subunit of the AMPA receptors via phosphorylation of GluA2 [23]. Proteomic analyses of adult mouse synaptic fractions led to the identification of DPYSL5 among the 1000 and more components of these large multi-proteins complexes [24]. Using total protein lysates from mouse brain at different developmental stages (postnatal day 14, 21 and adult), we also found that DPYSL5 was present in synaptic fractions extracted from cortex, cerebellum, hippocampus and striatum, in both pre-synaptic and postsynaptic fractions (Fig. 3, Supplementary Methods).

To evaluate the impact of the DPYSL5 genetic alteration on neuronal maturation and synaptic density, we focused our study on the analysis of the variants located in the N-terminal part of DPYSL5, including the previous published p.(Glu41Lys) and p.(Gly47Arg), and the novel recurrent p.(Glu25Lys) variant. Mature primary neuronal cultures were transfected and the density and maturity morphotype of the dendritic spines were assessed using immunocytochemistry and confocal microscopy. Interestingly, our experiments revealed that overexpression of DPYSL5-WT significantly increases synaptic density, compared to neurons expressing GFP alone, suggesting a promoting effect of DPYSL5 on synapse formation (Fig. 4A, B). This impact is also found in neurons expressing the p.(Glu41Lys) and p.(Gly47Arg) variants, but is absent when p.(Glu25Lys) variant is overexpressed. These results indicate that the p.(Glu41Lys) and p.(Gly47Arg) variants act similarly to DPYSL5-WT, unlike the p.(Glu25Lys) variant which had no effect on synapse formation, suggesting a loss of function impact (Fig. 4A, B). More specifically, when we looked at the morphotype of the dendritic spines in order to determine their maturity status, we found an increased density of mature spines, but not immature spines, in neurons overexpressing DPYSL5-WT or p.(Glu25Lys) variants (Fig. 4C–E). The p.(Gly47Arg) variant caused an increased density of immature spines (filopodia) and a decreased density of mature spines, and the p.(Glu41Lys) variant was only associated with a decreased density of mature spines (Fig. 4C–E).

### Abnormal neurite outgrowth processes in <sup>WT/p.(Glu41Lys)</sup> human iPSC-derived neural stem cells

To provide additional evidence regarding the direct impact of DPYSL5 on neuronal development, we established a human neuronal model that endogenously expresses the recurrent variant p.(Glu41Lys) in the heterozygous state. The interest of this approach was to evaluate the specific impact of the heterozygous nucleotide substitution, expressed at the endogenous level, on neuronal developmental processes. Importantly, this human neuronal model would provide molecular data that can be compared with the results obtained using the primary neuronal cultures overexpressing the p.(Glu41Lys) variant following plasmid transfection. We used the control human iPSC (hiPSC) line (ASE-9211), from a male individual, in which we performed CRISPR/Cas9 genome editing to integrate the heterozygous missense variant. The nucleotide substitution was

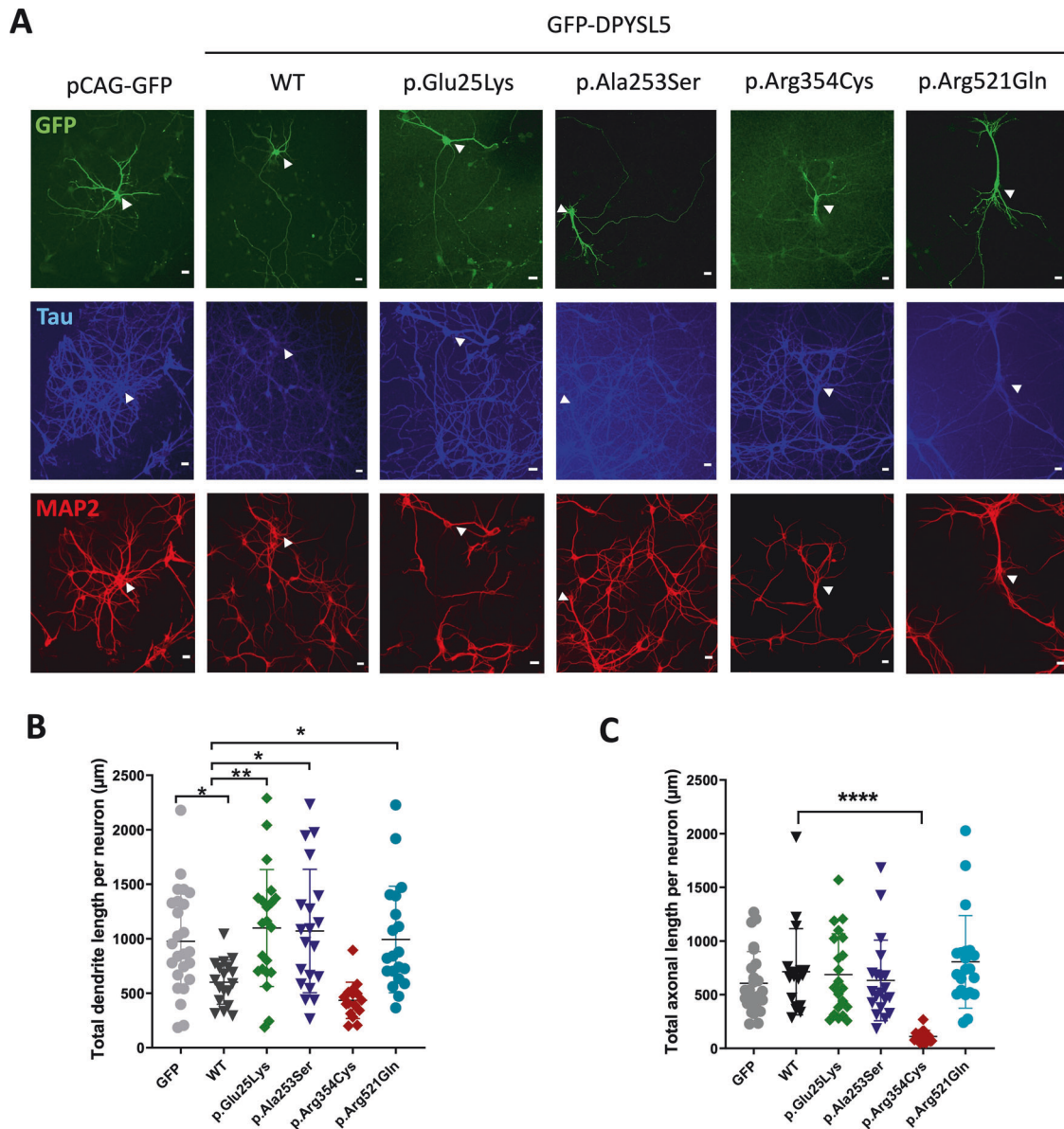


**Fig. 2** The candidate DPYSL5 variants impair neurite development in vitro. **A** Confocal microscopy images of neurons at 7 days of in vitro culture (DIV) transfected at DIV4 with pCAG-GFP, WT-GFP-DPYSL5, p.Glu25Lys-GFP-DPYSL5, p.Ala253Ser-GFP-DPYSL5, p.Arg354Cys-GFP-DPYSL5, p.Glu370Gly-GFP-DPYSL5, p.Arg521Gln-GFP-DPYSL5 and labeled with anti-Tau (axon, in blue) and anti-MAP2 (dendrites, in red) antibodies. The arrowhead shows the cell bodies of neurons transfected with the plasmids pCAG-GFP, WT or mutated forms of DPYSL5. Scale bar: 20  $\mu\text{m}$ . **B, C** Quantification of total dendritic (B) and axonal (C) length. Each plot in the graph corresponds to one analyzed neuron. Four independent transfections and more than 15 neurons were analyzed for each group. ANOVA Kruskal–Wallis test and Dunn’s multiple comparisons test were used. Data are expressed as mean  $\pm$  SD. SD standard deviation, Ns not significant, \*  $p < 0.05$ ; \*\* $p < 0.01$ ; \*\*\*  $p < 0.001$ ; \*\*\*\* $p < 0.0001$ .

validated by Sanger sequencing (Supplementary Fig. 3). We obtained two clones with the  $\text{WT/p.(Glu41Lys)}$  genotype and their genomic integrity was also validated by digital PCR-based assays (Stem Genomics). The WT and  $\text{WT/p.(Glu41Lys)}$  hiPSC lines were then differentiated into neural stem cells (NSC) to obtain 3 clones for each genotype (Fig. 5A). The efficiency of the NSC induction was validated by immunostaining of SOX2 and Nestin antibodies (Supplementary Fig. 4), with that at least 80% of the hiPSC-derived NSC positive for SOX2 and for Nestin. The endogenous DPYSL5 protein expression level was similar for both WT and  $\text{WT/p.(Glu41Lys)}$  hiPSC and NSC cells, suggesting that the mutation does not alter protein stability (Fig. 5B, Supplementary Fig. 5). We next tested the viability and proliferation of  $\text{WT/p.(Glu41Lys)}$  NSC cultures compared to the WT NSC and the data were similar in

both genotypes, indicating that the heterozygous p.(Glu41Lys) variant does not alter culture growth and cell replication (Supplementary Fig. 6). We then focused our analyses on the morphology of the differentiated NSC by measuring the total length of the neurites stained by an antibody specific to the MAP2 protein (Fig. 5C). Our experiments revealed that the  $\text{WT/p.(Glu41Lys)}$  NSC showed a significant increased total length of neurites per cell, when compared to the data on the WT NSC (Fig. 5D), which confirms that this variant is responsible for the impaired regulatory function of DPYSL5 on neurite and dendrite outgrowth. Moreover, these findings replicate our results obtained in primary developing neurons that transiently overexpressed the p.(Glu41Lys) variant, which suggest that this model is relevant and can be used to assess candidate DPYSL5 variants.

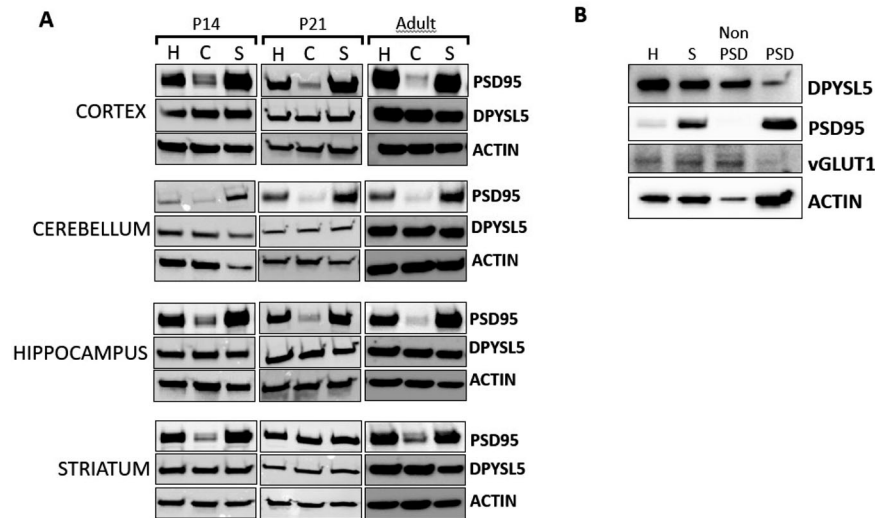


**Fig. 3 Expression analysis of endogenous DPYSL5 protein in developing mouse brain and in synaptic fractions.** **A** Expression analysis of DPYSL5 protein in lysates of mouse cortex, cerebellum, hippocampus and striatum at different stages of development (postnatal day P14, P21 or adult). The DPYSL5 protein (62 kDa) expression was detected by SDS-PAGE and immunoblotting using an anti-DPYSL5 antibody and the PSD95 protein was used as a control for the enrichment of synaptic proteins in subcellular fractionation. Actin protein was used as a loading reference. H Homogenate, C cytoplasm, S synaptic fraction. **B** Analysis of DPYSL5 protein expression after subcellular separation of the presynaptic (Non PSD) and postsynaptic (PSD) fractions in mouse adult cortex. H Homogenate, S Synaptoneurosomes, PSD postsynaptic density.

## DISCUSSION

The *DPYSL5* gene has been recently described as a novel candidate for NDDs and brain malformations, through the identification of a de novo p.(Glu41Lys) variant in eight unrelated subjects with ID, corpus callosum agenesis and posterior fossa abnormalities, as well as a p.(Gly47Arg) variant in an individual with Ritscher-Schinzel syndrome [8]. Our study expands the number of *DPYSL5* variants associated with neurodevelopmental disorders with or without brain malformations through the analysis of 9 additional families, as well as contributing functional evidence of their deleterious impact on neuronal development using in vitro mouse and human neuronal cultures.

### *DPYSL5* variants define a distinct neurodevelopmental syndrome

Although we identified a heterozygous *DPYSL5* variant in one of the two sisters originally reported in the first description of Ritscher-Schinzel syndrome, detailed phenotypic comparison supports the delineation of a distinct neurodevelopmental disorder [8]. Ritscher-Schinzel syndrome is typically defined by a triad of craniofacial dysmorphism, cerebellar malformations, and congenital heart defects. Additional clinical features may include limbs anomalies, cleft palate, and ocular defects such as coloboma.

Individuals with deleterious missense variants in *DPYSL5* present with a partially overlapping but distinct phenotype. While cerebellar hypoplasia and neurodevelopmental delay are observed in both conditions, the *DPYSL5*-related disorder is characterized by the frequent presence of corpus callosum agenesis, movement disorders, epilepsy, and behavioral disorders—features not typically reported in Ritscher-Schinzel syndrome. Conversely, congenital heart defects and characteristic craniofacial features of Ritscher-Schinzel syndrome are notably absent in individuals with *DPYSL5* variants.

### The N-terminal DPYSL5 missense variants p.(Glu41Lys) and p.(Glu25Lys) are strongly associated with NDD and ACC

We confirmed the contribution of the p.(Glu41Lys) recurrent variant, with the description of two additional individuals (one child and one fetus) with ACC. We also identified a second recurrent de novo variant, p.(Glu25Lys), in three individuals (two fetuses, one child) of our series, all presenting with ACC. It is

therefore critical to note that most of the individuals with *DPYSL5* variants had brain malformations (7/9), including ACC, which is a neuroanatomical malformation that is also associated with other genetic forms with NDD [25–27]. Moreover, our study reveals that the two recurrent variants, p.(Glu41Lys) and p.(Glu25Lys), are recurrently associated with ACC. Interestingly, ACC has been described in individuals with a de novo missense variant in *DPYSL2*, suggesting that genes of the DPYSL family are crucial for brain development [9]. Importantly, our results, which include data from prenatal genetic testing and fetal brain imaging, provide important insights for prenatal diagnosis and genetic counseling.

It also appears that the missense variants, when located in the N-terminal part of DPYSL5, are strongly associated with NDD and ACC, whereas the other variants included in central or in C-terminal domains of the protein are found in individuals with a mild phenotype and without ACC. These findings would indicate a relative clinical and molecular heterogeneity that could be considered for genetic diagnosis and counseling when a missense variant of DPYSL5 outside the N-terminal domain is identified in an individual with NDD.

Interestingly, both recurrent mutations (*i.e.* p.Glu25Lys or p.Glu41Lys) target surface-exposed residues located close to each other at the N-terminal part of DPYSL5 protein (glutamic acid at positions 25 or 41) (Fig. 1). We previously demonstrated that the p.(Glu41Lys) variant decreased the physical interaction between DPYSL5 and the cytoskeleton-associated proteins TUBB3 and MAP2, which are essential for its inhibitory regulation of dendritic elongation [8]. As an increased dendritic growth was also observed in neurons overexpressing p.(Glu25Lys)-DPYSL5, similarly to the p.(Glu41Lys) variant, it is likely that a N-terminal DPYSL5 protein sequence including Glu25 and Glu41 residues define a functional domain for DPYSL5 regulation of dendritic elongation, although we found that only the p.(Glu41Lys) variant, and not p.(Glu25Lys), impair the interaction between DPYSL5 and cytoskeleton-associated proteins. This result suggests that another pathophysiological mechanism, independent of DPYSL5-cytoskeleton interaction, would occur during brain development.

### DPYSL5 candidate variants outside the N-terminal region may impair DPYSL5 structure and phosphorylation

The missense variants located outside the N-terminal region may be involved in DPYSL5 structure or function. Indeed, the p.(Arg231His)

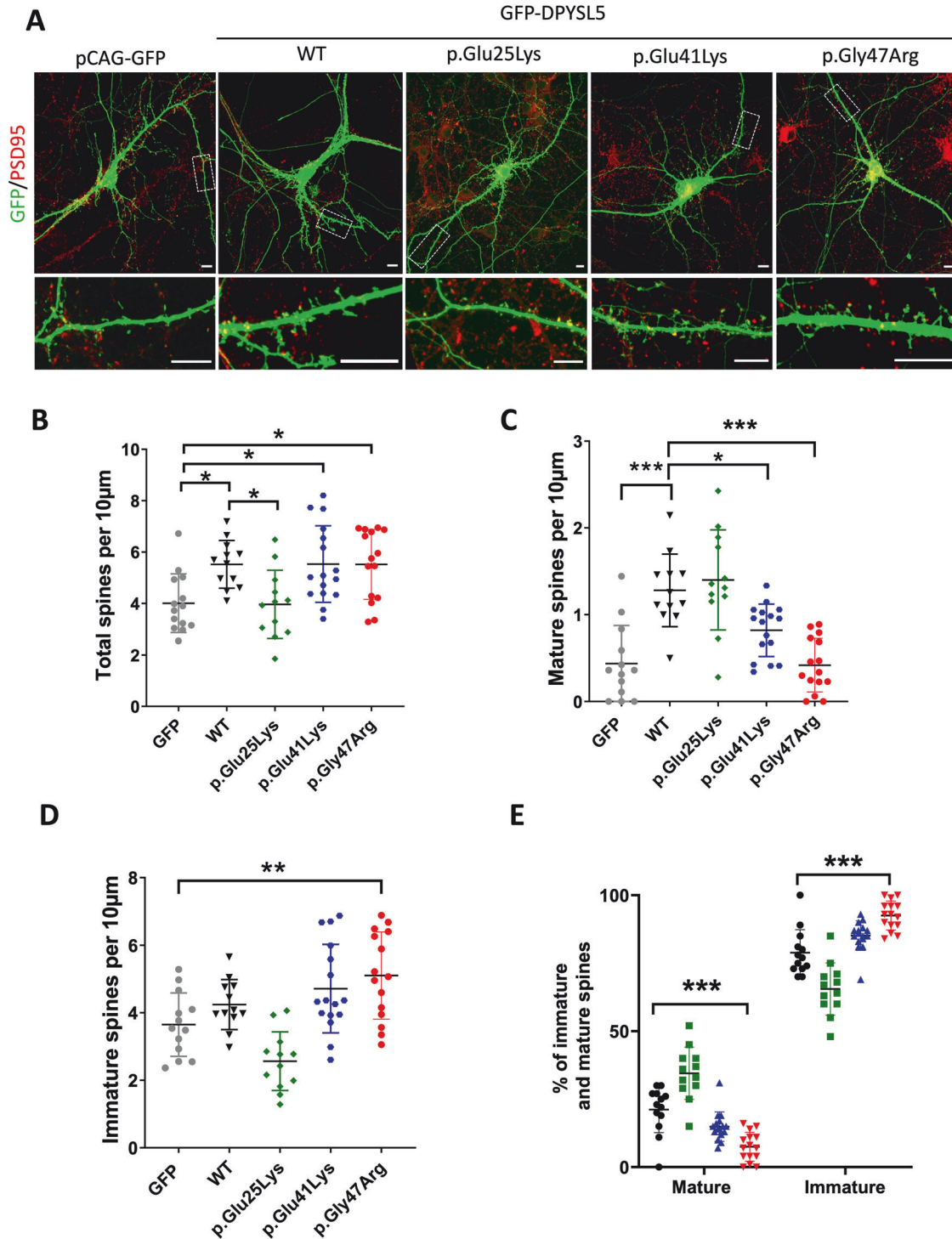


**Fig. 4** Altered spine density or synapse maturity in primary hippocampal neurons overexpressing the de novo N-terminal DPYSL5 variants. **A** Representative confocal microscopy images of mature hippocampal primary neuronal cultures transiently transfected with pCAG-GFP, WT-GFP-DPYSL5, p.Glu25Lys-GFP-DPYSL5, p.Glu41Lys-GFP-DPYSL5, p.Gly47Arg-GFP-DPYSL5. The GFP labeling was used to display spine morphology and a PSD95 antibody was used for labeling mature dendritic spines (in red). Scale bar: 20 μm. **B** Quantification of synaptic density (number of spines per 10 μm of dendrite) for each condition, 10–20 neurons were analyzed. ANOVA Kruskal-Wallis test and Turkey's multiple comparisons test, data are expressed as mean ± SD. SD, standard deviation; \* $p < 0.05$ . **C** Quantification of the density of mature spines. Mature spines were differentiated according to their head diameter ( $>0.6 \mu\text{m}$  for mature spines) coupled with the presence of PSD95 marking. Three independent transfections, 10–20 neurons analyzed, ANOVA Kruskal-Wallis test and Turkey's multiple comparisons test, data are expressed as mean ± SD. \*\* $p < 0.01$  \*\*\* $p < 0.001$ . **D** Quantification of immature spines density. Immature spines were defined with the head diameter  $<0.6 \mu\text{m}$  and absence of PSD95 marking. Three independent experiments, 10–20 neurons were analyzed and compared to WT, ANOVA Kruskal-Wallis test and Turkey's multiple comparisons test. Mean ± SD are represented on the graph. \*\* $p < 0.01$ . **E** Graphic representation of the ratio of mature/immature spines. Three independent experiments, 10–15 neurons were analyzed for each condition. The ratio of mature to immature spines for each variant was compared to the ratio of neurons overexpressing the DPYSL5-WT. Kruskal Wallis test and Dunn's multiple comparisons test. Data represented Mean ± SD. SD, Standard deviation; \*\*\* $p < 0.001$ .

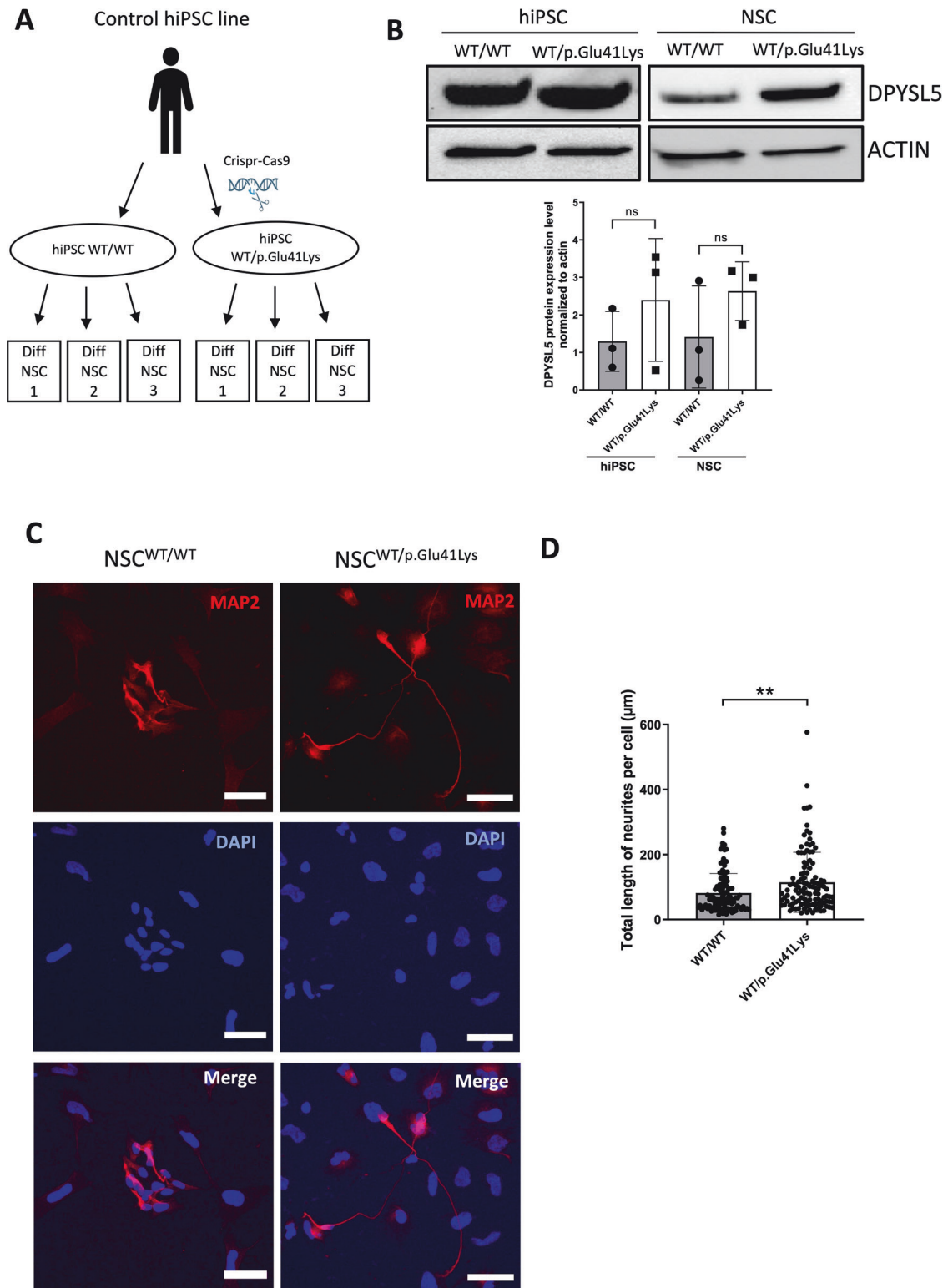


**Fig. 5** Neurite outgrowth is increased in human Neural Stem Cells heterozygous for the recurrent p.(Glu41Lys) variant. **A** Schematic representation of the study design. Example demonstrating how each clone hiPSC clone was used to derive multiple NSC lines. **B** Immunoblotting using anti-DPYSL5 antibody and the actin protein was used as a reference in both hiPSC lines and NSC. Quantification of DPYSL5 protein expression was performed on three independent cultures or differentiations from hiPSC, and measurements were normalized to actin expression level. Mann-Whitney test, data are expressed as mean  $\pm$  SD. SD, standard deviation; Ns, not significant. **C** Representative immunocytochemistry images of WT/WT and WT/p.Glu41Lys NSC. Differentiating NSC were grown on glass coverslips and immunostaining with MAP2 antibody was realized 48 h after plating. Scale bar: 50  $\mu$ m. **D** Quantification of the total length of neurites per cells with MAP2 immunostaining in control and in WT/p.Glu41Lys NSC. Neurite length was measured on three NSC differentiations for each condition, each plot corresponding to one NSC. 110–120 cells were analyzed and the data presented as mean  $\pm$  SD. SD Standard deviation. Mann Withney test. \*\* $p < 0.01$ .

and p.(Ala253Ser) variants affect residues located in the central pocket of the DPYSL5 dimer (Fig. 1). However, DPYSL2 functions as a monomer to promote tubulin polymerization, which suggests that multimerization might not be needed for DPYSL proteins' biological function. In other studies, the residues 105–285 were essential for DPYSL5 localization to mitochondria which was integral to promoting mitophagy and reduced mitochondria number in neurons [28]. The p.(Arg231His) and p.(Ala253Ser) variants overlap with this domain and more specifically the p.(Ala253Ser) is directly localized the hydrophobic domain (residues 239–260) thought to facilitate DPYSL5 embedding into the mitochondrial membrane [28]. This suggests that p.(Ala253Ser) variant might affect bioenergetics of neurons and impair the removal of damaged mitochondria through mitophagy.

The p.(Arg521Gln) variant is within the known C-terminal tubulin-binding domain (residues 475–522) [10]. This variant is localized next to the phosphorylation site at Threonine 516 by Glycogen synthase kinase 3 beta (GSK3 $\beta$ ) which controls DPYSL5 function in neurite outgrowth [11]. This variant is also in the vicinity of another phosphorylation site by ataxia-telangiectasia disease protein ATM (position Serine538) which impairs DPYSL5 function [29]. While the p.(Arg521Gln) variant did not affect DPYSL5 binding to MAP2, TUBB3 or DPYSL2, it might affect DPYSL5 phosphorylation at either Threonine516 or Serine538 and its function as a blocker of neurite outgrowth.

#### DPYSL5 candidate variants outside the N-terminal region present in general population samples: consideration for genetic diagnosis

The p.(Arg521Gln), p.(Arg354Cys) and p.(Arg231His) variants, identified in patients with NDD and without ACC, are present in the recently updated gnomAD datasets at ultra-rare frequency and enriched in individuals from UKBiobank, suggesting an incomplete, reduced penetrance or a variable expressivity, which has been previously described in neurodevelopmental disorders [30–32]. Interestingly, a recent study assessed the role of genetic modifiers of rare variants in 599 genes involved in neurodevelopmental disorders, including *DPYSL5*, in the UKBiobank population cohort (419,854 participants) [33]. The results showed that approximately 12% of participants carry a rare predicted damaging variant in one of the 599 genes, and a further 1% carry a rare predicted damaging variant in more than one of these genes, conferring a higher risk of impaired cognitive performance and neuropsychiatric conditions [33].

In our study, the identification and functional characterization of the de novo p.(Arg354Cys) variant in *DPYSL5* indicate that it is deleterious, and associated with a decreased protein expression level. When considering the p.(Arg521Gln) and the p.(Arg231His) variants, the identification of additional patients carrying these variants could provide further insight into the pathogenicity level, as well as the associated penetrance and expressivity.

#### DPYSL proteins family, brain development and neurodevelopmental disorders

The Dihydropyrimidinase-like (DPYSL) proteins, which were initially identified as effectors of semaphorin 3 A signaling that regulates growth cone collapse [34], play important functions in mammalian brain development and function, such as neuronal migration, neurite extension, axonal guidance, dendritic spine development and synaptic plasticity [7]. Furthermore, transcriptomic data from the Allen Brain Atlas have established that the expression of the five *DPYSL* genes are high during prenatal and perinatal stages in the developing human brain [35]. Various genetic studies demonstrated the contribution of *DPYSL1*, *DPYSL2* and *DPYSL3* missense variants in the pathophysiology of NDDs [7, 36–40]. Particularly, ACC and NDD were also described in individuals with a de novo missense variant in *DPYSL2* [9]. This observation was of particular interest because *DPYSL2* and *DPYSL5* proteins play pivotal competitive roles during

early neuronal development in the modulation of dendrite outgrowth promotion, depending on their respective phosphorylation status. While *DPYSL2* phosphorylation disrupts its interaction with tubulin leading to growth inhibition, *DPYSL5* phosphorylation by GSK3 $\beta$  at Thr516 increases its binding to tubulin which prevents tubulin polymerization and block dendritic growth [41]. Consequently, the fine regulation of neuronal early development, through axonal elongation and dendritic outgrowth, that is driven by the competitive action of *DPYSL2* and *DPYSL5* proteins would be an essential physiological process in the formation of the corpus callosum, and also for brain development, maturation and cognition.

In summary, the expanded number of de novo *DPYSL5* variants reported in the present study provide additional findings on the clinical phenotypic spectrum, and suggest that brain abnormalities, including ACC, would be linked to variants in the N-terminal part of *DPYSL5* protein. We also report new findings from prenatal genetic testing and fetal brain imaging that provide important insights for prenatal diagnosis and genetic counseling. In general, the clinical and genetic data reported in our study have major implications for the diagnosis and clinical management of patients with a *DPYSL5* variant. Our findings also provide additional molecular evidence that would be of interest when studying into details the *DPYSL5*-associated pathophysiological mechanisms in relevant neuronal cellular and mouse models, and particularly for the recurrent variants.

#### DATA AVAILABILITY

The authors confirm that the data supporting the findings of this research are available within the manuscript or available upon request.

#### REFERENCES

- Zablotsky B, Black LI, Maenner MJ, Schieve LA, Danielson ML, Bitsko RH, et al. Prevalence and trends of developmental disabilities among children in the United States: 2009–2017. *Pediatrics*. 2019;144:e20190811.
- Kochinke K, Zweier C, Nijhof B, Fenckova M, Cizek P, Honti F, et al. Systematic phenomics analysis deconvolutes genes mutated in intellectual disability into biologically coherent modules. *Am J Hum Genet*. 2016;98:149–64.
- Klingler E, Francis F, Jabaudon D, Cappello S. Mapping the molecular and cellular complexity of cortical malformations. *Science*. 2021;371:eaba4517.
- Haldipur P, Millen KJ, Aldinger KA. Human cerebellar development and transcriptomics: implications for neurodevelopmental disorders. *Annu Rev Neurosci*. 2022;45:515–31.
- Hofman J, Hutny M, Sztuba K, Paprocka J. Corpus callosum agenesis: an insight into the etiology and spectrum of symptoms. *Brain Sci*. 2020;10:625.
- Edwards TJ, Sherr EH, Barkovich AJ, Richards LJ. Clinical, genetic and imaging findings identify new causes for corpus callosum development syndromes. *Brain*. 2014;137:1579–613.
- Desprez F, Ung DC, Vourc'h P, Jeanne M, Laumonier F. Contribution of the dihydropyrimidinase-like proteins family in synaptic physiology and in neurodevelopmental disorders. *Front Neurosci*. 2023;17:1154446.
- Jeanne M, Demory H, Moutal A, Vuillaume ML, Blesson S, Thépault RA, et al. Missense variants in *DPYSL5* cause a neurodevelopmental disorder with corpus callosum agenesis and cerebellar abnormalities. *Am J Hum Genet*. 2021;108:951–61.
- Suzuki H, Li S, Tokutomi T, Takeuchi C, Takahashi M, Yamada M, et al. De novo non-synonymous *DPYSL2* (CRMP2) variants in two patients with intellectual disabilities and documentation of functional relevance through zebrafish rescue and cellular transfection experiments. *Hum Mol Genet*. 2022;31:4173–82.
- Brot S, Rogemond V, Perrot V, Chounlamounri N, Auger C, Honnorat J, et al. CRMP5 interacts with tubulin to inhibit neurite outgrowth, thereby modulating the function of CRMP2. *J Neurosci*. 2010;30:10639–54.
- Brot S, Smaoune H, Youssef-Issa M, Mallevat C, Benetollo C, Besançon R, et al. Collapsin response-mediator protein 5 (CRMP5) phosphorylation at threonine 516 regulates neurite outgrowth inhibition. *Eur J Neurosci*. 2014;40:3010–20.
- Sobreira N, Schiettecatte F, Valle D, Hamosh A. GeneMatcher: a matching tool for connecting investigators with an interest in the same gene. *Hum Mutat*. 2015;36:928–30.
- Kircher M, Witten DM, Jain P, O'Roak BJ, Cooper GM, Shendure J. A general framework for estimating the relative pathogenicity of human genetic variants. *Nat Genet*. 2014;46:310–5.

14. Ioannidis NM, Rothstein JH, Pejaver V, Middha S, McDonnell SK, Baheti S, et al. REVEL: an ensemble method for predicting the pathogenicity of rare missense variants. *Am J Hum Genet.* 2016;99:877–85.
15. Cheng J, Novati G, Pan J, Bycroft C, Žemgulytė A, Applebaum T, et al. Accurate proteome-wide missense variant effect prediction with AlphaMissense. *Science.* 2023;381:eadg7492.
16. Alirezaie N, Kernohan KD, Hartley T, Majewski J, Hocking TD. ClinPred: prediction tool to identify disease-relevant nonsynonymous single-nucleotide variants. *Am J Hum Genet.* 2018;103:474–83.
17. Freeman PJ, Hart RK, Gretton LJ, Brookes AJ, Dagleish R. VariantValidator: accurate validation, mapping, and formatting of sequence variation descriptions. *Hum Mutat.* 2018;39:61–8.
18. Ung DC, Iacono G, Méziane H, Blanchard E, Papon MA, Selten M, et al. Ptchd1 deficiency induces excitatory synaptic and cognitive dysfunctions in mouse. *Mol Psychiatry.* 2018;23:1356–67.
19. Williams M, Prem S, Zhou X, Matteson P, Yeung PL, Lu CW, et al. Rapid detection of neurodevelopmental phenotypes in human neural precursor cells (NPCs). *J Vis Exp.* 2018;133:56628.
20. Berry KP, Nedivi E. Spine dynamics: are they all the same? *Neuron.* 2017;96:43–55.
21. Richards S, Aziz N, Bale S, Bick D, Das S, Gastier-Foster J, et al. Standards and guidelines for the interpretation of sequence variants: a joint consensus recommendation of the American College of Medical Genetics and Genomics and the Association for Molecular Pathology. *Genet Med.* 2015;17:405–24.
22. Ponnusamy R, Lohkamp B. Insights into the oligomerization of CRMPs: crystal structure of human collapsing response mediator protein 5. *J Neurochem.* 2013;125:855–68.
23. Lin Y-S, Lin Y-F, Chen KC, Yang YK, Hsiao Y-H. Collapsin response mediator protein 5 (CRMP5) causes social deficits and accelerates memory loss in an animal model of Alzheimer's disease. *Neuropharmacology.* 2019;157:107673.
24. Collins MO, Husi H, Yu L, Brandon JM, Anderson CN, Blackstock WP, et al. Molecular characterization and comparison of the components and multiprotein complexes in the postsynaptic proteome. *J Neurochem.* 2006;97:16–23.
25. Halgren C, Kjaergaard S, Bak M, Hansen C, El-Schich Z, Anderson CM, et al. Corpus callosum abnormalities, intellectual disability, speech impairment, and autism in patients with haploinsufficiency of ARID1B. *Clin Genet.* 2012;82:248–55.
26. Nabais Sá MJ, Venselaar H, Wiel L, Trimouille A, Lasseaux E, Naudion S, et al. De novo CLTC variants are associated with a variable phenotype from mild to severe intellectual disability, microcephaly, hypoplasia of the corpus callosum, and epilepsy. *Genet Med.* 2020;22:797–802.
27. Qi C, Feng I, Costa AR, Pinto-Costa R, Neil JE, Caluseriu O, et al. Variants in ADD1 cause intellectual disability, corpus callosum dysgenesis, and ventriculomegaly in humans. *Genet Med.* 2022;24:319–31.
28. Brot S, Auger C, Bentata R, Rogemond V, Ménigoz S, Chounlamountri N, et al. Collapsin response mediator protein 5 (CRMP5) induces mitophagy, thereby regulating mitochondrion numbers in dendrites. *J Biol Chem.* 2014;289:2261–76.
29. Reichlmeir M, Duecker RP, Röhrich H, Key J, Schubert R, Abell K, et al. The ataxia-telangiectasia disease protein ATM controls vesicular protein secretion via CHGA and microtubule dynamics via CRMP5. *Neurobiol Dis.* 2024;203:106756.
30. Niemi MEK, Martin HC, Rice DL, Gallone G, Gordon S, Kelemen M, et al. Common genetic variants contribute to risk of rare severe neurodevelopmental disorders. *Nature.* 2018;562:268–71.
31. Kingdom R, Wright CF. Incomplete penetrance and variable expressivity: from clinical studies to population cohorts. *Front Genet.* 2022;13:920390.
32. de Masfrand S, Cogné B, Nizon M, Deb W, Goldenberg A, Lecoquierre F, et al. Penetrance, variable expressivity and monogenic neurodevelopmental disorders. *Eur J Med Genet.* 2024;69:104932.
33. Kingdom R, Beaumont RN, Wood AR, Weedon MN, Wright CF. Genetic modifiers of rare variants in monogenic developmental disorder loci. *Nat Genet.* 2024;56:861–8.
34. Goshima Y, Nakamura F, Strittmatter P, Strittmatter SM. Collapsin-induced growth cone collapse mediated by an intracellular protein related to UNC-33. *Nature.* 1995;376:509–14.
35. Sunkin SM, Ng L, Lau C, Dolbeare T, Gilbert TL, Thompson CL, et al. Allen Brain Atlas: an integrated spatio-temporal portal for exploring the central nervous system. *Nucleic Acids Res.* 2013;41:D996–D1008.
36. Ravindran E, Arashiki N, Becker LL, Takizawa K, Lévy J, Rambaud T, et al. Mono-allelic CRMP1 gene variants cause neurodevelopmental disorder. *Elife.* 2022;11:e80793.
37. Satterstrom FK, Kosmicki JA, Wang J, Breen MS, De Rubeis S, An JY, et al. Large-scale exome sequencing study implicates both developmental and functional changes in the neurobiology of autism. *Cell.* 2020;180:568–584.e23.
38. Iossifov I, O'Roak BJ, Sanders SJ, Ronemus M, Krumm N, Levy D, et al. The contribution of de novo coding mutations to autism spectrum disorder. *Nature.* 2014;515:216–21.
39. De Rubeis S, He X, Goldberg AP, Poultnery CS, Samocha K, Cicek AE, et al. Synaptic, transcriptional and chromatin genes disrupted in autism. *Nature.* 2014;515:209–15.
40. Tsutiya A, Nakano Y, Hansen-Kiss E, Kelly B, Nishihara M, Goshima Y, et al. Human CRMP4 mutation and disrupted Crmp4 expression in mice are associated with ASD characteristics and sexual dimorphism. *Sci Rep.* 2017;7:16812.
41. Yamashita N, Goshima Y. Collapsin response mediator proteins regulate neuronal development and plasticity by switching their phosphorylation status. *Mol Neurobiol.* 2012;45:234–46.

## ACKNOWLEDGEMENTS

We deeply thank the patients and their families for their participation to the study. The authors also thank the "IBiSA Electron Microscopy Facility" of the University of Tours for management and access to the confocal microscopy platform, and Dr Marie-Laure Vuillaume-Winter for her valuable advice on variant classification. We thank Dr Stéphanie Bigou from the ICV-iPS core facility of the Paris Brain Institute (ICM).

## AUTHOR CONTRIBUTIONS

Conceptualization: A.M., M.J., F.L.; Formal Analysis: F.D., S.R., S.M., L.F.-M., A.M., F.L.; Funding Acquisition: A.M., F.L.; Investigation: F.D., S.R., L.F.-M., J.K., K.L., B.K., J.-M. de S.-A., C.P., G.M., K.A., E.P., G.L., V.R., C.F., W.K., D.L., S.G., I.G., W.C., J.C.H., O.B., C.K., S.U.; Methodology: F.D., S.R., L.F.-M., D.U., A.D., S.M., A.M., F.L.; Resources: L.F.-M., D.U., A.D., J.K., K.L., B.K., J.-M. de S.-A., C.P., G.M., K.A., E.P., G.L., V.R., C.F., W.K., D.L., S.G., A.T., I.G., W.C., J.C.H., O.B., C.K., S.U., A.M., F.L.; Project administration: A.M., M.J., F.L.; Visualization: F.D., S.R., A.M., F.L.; Supervision: A.M., M.J., F.L.; Writing-original draft, review and editing: F.D., S.R., J.K., W.C., A.M., M.J., F.L.

## FUNDING

This study was funded by the Association pour le Développement de la Neurogénétique (ADN), the Fédération Hospitalo-Universitaire (FHU) GenoMedS, and by the Inserm (Cross-cutting program "GOLD" on genomic variability), to F. Laumonnier. Research reported in this publication was also supported by startup funds from Saint Louis university, National Institutes of Health NINDS R01NS119263 and R01NS119263-04S1 (to A. Moutal); NINDS R21NS137054-01 (to L. François-Moutal); U.S. NHGRI UM1HG007301 grant (Clinical Sequencing Exploratory Research Consortium, to W.V. Kelley, C.R. Finnila and D.R. Latner); Jordan's Guardian Angels, the Sunderland Foundation and the Brotman Baty Institute (to G. M. Mirzaa). The ICV-iPS core facility of the Paris Brain Institute (ICM) has received funding from the program "Investissements d'avenir" ANR-10-IAIHU-06.

## ETHICS DECLARATION

Parents and legal guardians of all affected individuals gave their informed consent for the publication of clinical and genetic information, and the study was approved by the respective local ethics committees. The study complied with the principles set out in the Declaration of Helsinki. All mouse experiments were performed according to protocols approved by the French Ministry of research and by INSERM (Project authorization numbers 01456.03 and HC2021-03). The use of the hiPSC cell line ASE-9211 has been declared to the French ministry of Research (CODECOH reference number DC-2022-5113) and the generation of the edited <sup>WT/p.Glu41Lys</sup> hiPSC line is included in a regulatory approval from the Ministry of Research (DUO 7675).

## COMPETING INTERESTS

The authors declare no competing interests.

## ADDITIONAL INFORMATION

**Supplementary information** The online version contains supplementary material available at <https://doi.org/10.1038/s41380-025-03364-8>.

**Correspondence** and requests for materials should be addressed to Frédéric Laumonnier.

**Reprints and permission information** is available at <http://www.nature.com/reprints>

**Publisher's note** Springer Nature remains neutral with regard to jurisdictional claims in published maps and institutional affiliations.



**Open Access** This article is licensed under a Creative Commons Attribution 4.0 International License, which permits use, sharing, adaptation, distribution and reproduction in any medium or format, as long as you give appropriate credit to the original author(s) and the source, provide a link to the Creative Commons licence, and indicate if changes were made. The images or other third party material in this article are included in the article's Creative Commons licence, unless indicated otherwise in a credit line to the material. If material is not included in the article's Creative Commons licence and your intended use is not permitted by statutory regulation or exceeds the permitted use, you will need to obtain permission directly from the copyright holder. To view a copy of this licence, visit <http://creativecommons.org/licenses/by/4.0/>.

© The Author(s) 2025